Inorg. Chem. **1997,** *36,* 2969−2974

The mpz^+/$mpz^{\bullet}$ Pair as Organic Analogue of the NO^+/$NO^{\bullet}$ Ligand Redox System (mpz = *N*-Methylpyrazinium). A Combined Electrochemical and Spectroscopic Study (UV/Vis/NIR, IR, EPR) of Complexes $[(mpz)M(CN)_5]^{2-/3-}$ (M = Fe, Ru, Os)

Eberhard Waldhör and Wolfgang Kaim*

Institut für Anorganische Chemie, Universität Stuttgart, Pfaffenwaldring 55, D-70550 Stuttgart, Germany

José A. Olabe* and Leonardo D. Slep

Departamento de Química Inorgánica, Analítica y Química Física (Inquimae), Facultad de
Ciencias Exactas y Naturales, UBA, Pabellón 2, Ciudad Universitaria,
Buenos Aires, Capital Federal 1428, Republic of Argentina

Jan Fiedler

J. Heyrovsky Institute of Physical Chemistry, Academy of Sciences of the Czech Republic,
Dolejškova 3, CZ-182 23 Prague 8, Czech Republic

Received November 27, 1996[⊗]

The oxidation and reduction behavior of complexes $[(mpz)M(CN)_5]^{2-}$ between the group 8 pentacyanometalates(II) and the *N*-methylpyrazinium ion mpz^+ was studied using spectroelectrochemical techniques (UV/vis/NIR, IR, EPR) in nonaqueous and, in part, aqueous media. As a further source of information on the electronic structure, we studied the variable solvatochromism of MLCT absorption bands in the precursor ions $[(mpz)M(CN)_5]^{2-}$. The mpz-centered one-electron reduction showed a tendency for concomitant loss of cyanide (EC process) to yield ions $[(mpz)M(CN)_4]^{2-}$, the lability increasing in the order M = Os << Ru < Fe. In contrast to the EPR spectra obtained from reduction with $S_2O_4^{2-}$ in aqueous media, which showed no evidence for close $mpz^{\bullet}$/metal association, the *intra muros* electrolysis experiments in DMSO or acetonitrile yielded the following results: The EPR spectrum that was previously assigned to $[(mpz)Fe(CN)_5]^{3-}$ is now ascribed to $[(mpz)Fe(CN)_4]^{2-}$. Whereas the dissociatively inert osmium radical complex $[(mpz)Os(CN)_5]^{3-}$ is distinguished by a broad EPR signal with a rather large value $g_{iso} = 2.0157$, the EPR spectrum of $[(mpz)Ru(CN)_4]^{3-}$ reveals well-resolved separate coupling with the ^{99}Ru and ^{101}Ru isotopes in natural abundance. Spectroelectrochemistry and reactivity patterns of the complex ions $[(mpz)M(CN)_5]^{2-}$ are reminiscent of results for corresponding nitrosyl complexes $[(NO)M(CN)_5]^{2-}$, which suggests that the mpz^+/$mpz^{\bullet}$ ligand redox pair can function as an organic analogue of the NO^+/$NO^{\bullet}$ redox system.

Introduction

Few ligands in coordination chemistry carry a positive charge.[1−4] This observation can be ascribed to the situation in a coordinative bond which implies electron pair donation from the ligand L to the metal center M: $L^{\delta+} \rightarrow M^{\delta-}$. For positively charged ligands the unfavorable electrostatic situation from the σ donor contribution must be overcompensated by strong backdonation from an electron-rich metal center to low-lying molecular orbitals of the ligand. The prototypical monopositive ligand is nitrosylium cation NO^+, a good π acceptor ligand.[1] Occupation of the low-lying π^*(LUMO) level of NO^+ by one electron in either free or coordinated form leads to the nitrosyl radical, $NO^{\bullet}$, the chemistry of which has received an enormous boost recently due to the biological relevance of physiologically generated NO.[1b,5]

Another monopositive, monodentate ligand is the relatively small *N*-methylpyrazinium (mpz^+) cation, which is known to form fairly stable complexes, e.g. with Co(II),[2] Mo(0), W(0),[3] cationic or anionic Fe(II),[6] Ru(II),[7] and Os(II).[7b,8] mpz^+ is a very weak σ base ($pK_a \approx -6$) but a good π acceptor, showing unusually short N(mpz^+)−metal bonds to Ru(II)[7c] or W(0)[3a]

[⊗] Abstract published in *Advance ACS Abstracts,* May 15, 1997.

(1) (a) McCleverty, J. A. *Chem. Rev.* **1979**, *79*, 37. (b) Clarke, M. J.; Gaul J. B. *Struct. Bonding (Berlin)* **1993**, *81*, 147. (c) Feltham, R. D.; Enemark, J. M. *Top. Stereochem.* **1981**, *12*, 155.

(2) Darby, W. L.; Vallarino, L. M. *Inorg. Chim. Acta* **1983**, *75*, 65 and literature cited.

(3) (a) Bruns, W.; Hausen, H.-D.; Kaim, W., Schulz, A. *J. Organomet. Chem.* **1993**, *444*, 121. (b) Hilgers, F.; Bruns, W.; Fiedler, J.; Kaim, W. *J. Organomet. Chem.* **1996**, *551*, 273.

(4) For chelate ligands see: (a) Kaim, W.; Matheis, W. *Chem. Ber.* **1990**, *123*, 1323. (b) Matheis, W.; Kaim, W. *J. Chem. Soc., Faraday Trans.* **1990**, *86*, 3337. (c) Inoue, M. B.; Inoue, M.; Bruck, M. A.; Fernando Q. *J. Chem. Soc., Chem. Commun.* **1992**, 515.

(5) (a) Stamler, J. S.; Singel, D. J.; Loscalzo, J. *Science* **1992**, *258*, 1898. (b) Butler, A. R.; Williams, D. L. H. *Chem. Soc. Rev.* **1993**, 233.

(6) (a) Toma, H. E.; Malin, J. M. *Inorg. Chem.* **1973**, *12*, 1039. (b) Wohlers, H. D.; Tassel K. D.; Bowermann, B. A.; Petersen, J. D. *Inorg. Chem.* **1980**, *19*, 2837. (c) Eaton, D. R.; Watkins, J. M.; Buist, R. J. *J. Am. Chem. Soc.* **1985**, *107*, 5604.

(7) (a) Ford, P. D.; Rudd, D. P.; Gaunder, R.; Taube, H. *J. Am. Chem. Soc.* **1968**, *90*, 1187. (b) Creutz, C.; Chou, M. H. *Inorg. Chem.* **1987**, *26*, 2995. (c) Wishart, J. F.; Bino, A.; Taube, H. *Inorg. Chem.* **1986**, *25*, 3318. (d) Poppe, J.; Kaim, W.; Ben Altabef, A.; Katz, N. E. *J. Chem. Soc., Perkin Trans. 2* **1993,** 2105. (e) Johnson, C. R.; Shepherd, R. E. *Inorg. Chem.* **1983**, *22*, 1117. (f) Johnson, C. R.; Shepherd R. E. *Inorg. Chem.* **1983**, *22*, 2439. (g) Hoddenbagh, J. M. A.; Macartney, D. H. *Inorg. Chem.* **1986**, *25*, 2099. (h) Hoddenbagh, J. M. A.; Macartney, D. H. *Inorg. Chem.* **1986**, *25*, 380.

(8) Slep, L. D.; Baraldo, L. M.; Olabe, J. A. *Inorg. Chem.*, **1996**, *35*, 6327.

S0020-1669(96)01426-7 CCC: $14.00

Table 1. Electrochemical Data for the Complexes[a]

complex	E_{ox}	E_{red1}	E_{red2}	scan rate	medium[b]
$[(mpz)Fe(CN)_5]^{2-}$ [c]	0.12 (98)	−0.72 (irr)		0.1	CH_3CN/Bu_4NPF_6
	0.16 (130)	−0.75 (81)		5.0	CH_3CN/Bu_4NPF_6
$[(mpz)Fe(CN)_4]^{2-}$ [c,d]		−1.17 (120)		0.1	CH_3CN/Bu_4NPF_6
$[(mpz)Ru(CN)_5]^{2-}$ [c]	0.47 (128)	−0.96 (84)	−2.36 (irr)	0.1	CH_3CN/Bu_4NPF_6
$[(mpz)Os(CN)_5]^{2-}$ [c]	0.26 (84)	−1.10 (84)	−2.08 (irr)	0.1	CH_3CN/Bu_4NPF_6
$[(mpz)Fe(CN)_5]^{2-}$	0.61 (96)	−0.72 (irr)		5.0	H_2O/KCl, pH 7
	n.d.	−0.80 (68)		5.0	H_2O/KCl, pH 9.5
	n.d.	−0.74 (67)		0.1	H_2O/KCl, pH 14
$[(mpz)Ru(CN)_5]^{2-}$	1.00[e]	−0.71 (92)		5.0	H_2O/KCl, pH 7
$[(mpz)Os(CN)_5]^{2-}$	0.76 (102)	−0.71 (123)		5.0	H_2O/KCl, pH 1
	0.76 (81)	−0.75 (irr)		0.02	H_2O/KCl, pH 1
	0.77 (93)	−0.71 (93)		0.1	H_2O/KCl, pH 7
$[(NO)Fe(CN)_5]^{2-}$ [f]		−0.82 (irr)		0.08	CH_2Cl_2/Bu_4NPF_6
$[(NO)Ru(CN)_5]^{2-}$ [g]		−1.04		n.r.	CH_3CN/Bu_4NPF_6
$[(NO)Os(CN)_5]^{2-}$		−1.03			CH_3CN/Bu_4NPF_6

[a] From cyclic voltammetry. Potentials in V vs SCE; $E(SCE) = E(Ag/AgCl) - 0.02\ V = E(Fc^+/Fc) + 0.45\ V$. Peak potential differences in mV (in parentheses). Cathodic peak potentials given for irreversible (irr) reduction processes. Scan rates in V/s. [b] 0.1 M in supporting electrolyte.[c] 0.1 M [2.2.2]cryptand added for solubilizing. [d] Compound formed by cyanide dissociation (see Figure 1 and Scheme 1). [e] From ref 8. [f] From refs 14a and 15. [g] From ref 14b.

and being easily reduced to the *N*-methylpyrazinium radical mpz$^•$. Free mpz$^•$ is not very persistent as evident from electrochemical and EPR studies;[9] however, it can be stabilized through metal coordination[10] at the nitrogen donor site. EPR studies of such metal complexes of a "spin-labeled ligand"[6c] have appeared[3,6c,7d] and have revealed detailed effects of metal/ligand π bonding.[3,7c]

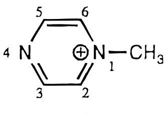

mpz^+

We report here on the redox systems $[(mpz)M(CN)_5]^{2-/3-}$, M = Fe, Ru, and Os. The iron system was reinvestigated because of discrepancies with respect to literature results;[6c] the 2− species of the ruthenium and osmium compounds were described earlier together with basic spectroscopic and kinetic data.[7e−h,8] Pentacyanometalate(II) fragments of the group 8 metals are π donating and are distinguished from the much-studied pentaammine analogues[7a−d] by the negative charge. The physical measurements used include cyclic voltammetry, IR and UV/vis/NIR absorption spectroscopy (including spectroelectrochemistry and solvatochromism), and high-resolution EPR spectroscopy of the paramagnetic reduced forms.

Experimental Section

Materials. $Na_2[(mpz)Fe(CN)_5]\cdot 4H_2O$ and $Na_2[(mpz)Os(CN)_5]\cdot 4H_2O$ were obtained according to literature procedures.[6a,8] All measurements involving reductions were carried out in dry solvents under an argon atmosphere. Sodium or potassium salts of the complexes were solubilized by adding an excess of [2.2.2]cryptand (about 0.1 M).

$K_2[(mpz)Ru(CN)_5]\cdot 2H_2O$. First, $K_2[Ru(CN)_5NO]\cdot H_2O$ was prepared as a starting material by the same technique as used for the osmium compound but with a shorter irradiation period of 20 h.[8] To 100 mL of an aqueous solution of the nitrosyl complex (70 mg) was added slowly concentrated ammonia up to pH 11. The mixture was held at 40 °C in a sealed flask during 10 h. Then it was cooled in an ice-bath, and 2 M HCl was added to reach pH 8. An excess of methylpyrazinium iodide[6a] (560 mg) was added, and the solution was heated at 40 °C during 2 h and then concentrated to 3−4 mL. Precipitation was obtained by adding a saturated solution of KI in ethanol. The solid was filtered off (frit No. 4), washed with ethanol and ether, and dried over P_2O_5. Anal. Calcd for $K_2[Ru(CN)_5(mpz)]\cdot 2H_2O$: C, 27.27; H, 2.52; N, 22.26. Found: C, 27.21; H, 2.13; N, 22.03.

Instrumentation. EPR spectra were recorded in the X band on a Bruker System ESP 300 equipped with a Bruker ER035M gaussmeter and a HP 5350B microwave counter. Infrared spectra were obtained using a Philips PU 9800 FTIR instrument. UV/vis/NIR absorption spectra were recorded on Shimadzu UV160 and Bruins Instruments Omega 10 spectrophotometers. Cyclic voltammetry was carried out in acetonitrile/0.1 M Bu_4NPF_6 or buffered H_2O/0.1 M KCl using a three-electrode configuration (glassy carbon working electrode, Pt counter electrode, Ag/AgCl reference) and a PAR 273 potentiostat and function generator. The ferrocene/ferrocenium couple $Fc^{+/0}$ was used as internal reference in acetonitrile. Potentials vs $Fc^{+/0}$ (in acetonitrile) and Ag/AgCl (in water) were converted to values vs SCE by adding 0.45 V and subtracting 0.02 V,[11] respectively. Spectroelectrochemical measurements were performed using an optically transparent thin-layer electrode (OTTLE) cell[12] for UV/vis (CH_3CN/0.1 M Bu_4NPF_6/0.1 M [2.2.2]cryptand) and IR spectra (DMF/0.1 M Bu_4NPF_6/0.1 M [2.2.2]-cryptand) and a two-electrode capillary for EPR studies in various media.[13] Elemental analyses (C, H, N) were performed with a Carlo Erba EA 1108 analyzer, at Inquimae.

Results and Discussion

Cyclic Voltammetry. The complex ions $[(mpz)M(CN)_5]^{2-}$ were studied in acetonitrile and in water at selected different pH values. The data are summarized in Table 1 together with those of some related compounds.[14,15] The cyclovoltammogram for M = Fe is shown in Figure 1.

The metal-based reversible oxidations follow the standard pattern found with the hexacyanometalate species,[11] i.e., E_{ox} increases in the order M = Fe < Os < Ru. In acetonitrile these potentials are shifted by about 0.5 V to lower values relative to the numbers for aqueous solution because of destabilization of the HOMO by interaction of the coordinated cyanide ligands with the weaker aprotic acceptor solvent.

The $[(mpz)Fe(CN)_5]^{2-}$ ion exhibits irreversible one-electron reduction behavior in acetonitrile at slow scan rates, ac-

---

[9] Rakowsky, T.; Dohrmann, J. K. *Ber. Bunsenges. Phys. Chem.* **1979**, *83*, 495.

[10] Kaim, W. *Coord. Chem. Rev.* **1987**, *76*, 187.

[11] Bard, A. J.; Parsons, R.; Jordan, J. *Standard Potentials in Aqueous Solutions*; IUPAC: Oxford, U.K., 1985.

[12] Krejcik, M.; Danek, M.; Hartl, F. *J. Electroanal. Chem. Interfacial Electrochem.* **1991**, 317, 179.

[13] Kaim, W.; Ernst S.; Kasack, V. *J. Am. Chem. Soc.* **1990**, *112*, 173.

[14] (a) Bowden, W. L.; Bonnar, P.; Brown, D. B.; Geiger, W. E. *Inorg. Chem.* **1977**, *16*, 41. (b) Fiedler, J. *Coll. Czech. Chem. Commun.* **1993**, *58*, 461.

[15] (a) Fiedler, J.; Masek, J. *Inorg. Chim. Acta* **1986**, *111*, 39. (b) Masek, J.; Maslova, E. *Coll. Czech. Chem. Commun.* **1974**, *39*, 2141.

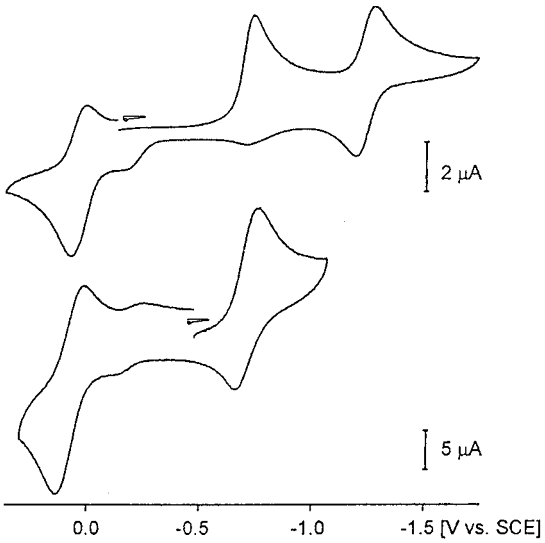

Figure 1. Cyclic voltammograms of $Na_2[(mpz)Fe(CN)_5]$ in CH_3CN/0.1 M Bu_4NPF_6/0.1 M [2.2.2]cryptand at 0.1 V/s (top) and 5.0 V/s scan rates (bottom).

Scheme 1

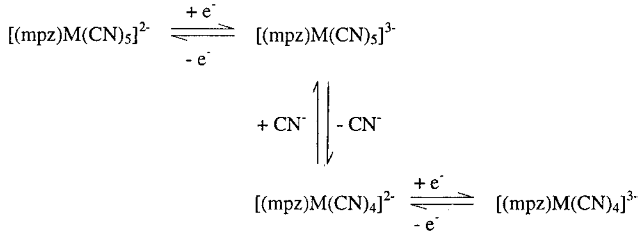

companied by the formation of a new species which is reversibly reduced at more negative potentials (Figure 1, Scheme 1). At higher scan rates, the primary reduction becomes reversible and the secondary reduction feature disappears. Identical observations were made in DMSO solution, where the iron complex is more soluble. The complexes of ruthenium and osmium are reversibly reduced by one electron even at slow scan rates; they exhibit an irreversible second reduction at very negative potentials.

The reduction behavior in aqueous solution is strongly pH-dependent, suggesting solvent interaction with the cyanide ligands. We thus studied the cyclic voltammetric response also in the presence of excess cyanide; the results in aprotic media had already suggested some cyanide dissociation (Scheme 1).[15]

In neutral aqueous solution and at scan rates up to 5 V/s the $[(mpz)Fe(CN)_5]^{2-}$ ion is irreversibly reduced. Addition of 0.5 M cyanide causes the appearance of an anodic counter peak at 5 V/s scan rate; a similar behavior is observed at 0.1 V/s when the measurement with added cyanide is performed in 1 M KOH. The $[(mpz)Ru(CN)_5]^{2-}$ ion exhibits quasi-reversible reduction behavior in neutral solution at 5 V/s scan rate and in the absence of additional cyanide; however, the cyclic voltammetric response is affected by electrode adsorption. In contrast, the osmium analogue is reversibly reduced even at slow scan rates such as 0.1 V/s in neutral solution; irreversibility occurs only in acidic solution (1 M HCl) at slow scan rates of 0.02 V/s or lower.

The first reduction potentials in acetonitrile follow the regular sequence M = Fe > Ru > Os, reflecting increasing back-donation from the metal center. There is less differentiation in aqueous solution due to dominating cyanide−solvent interaction. The patterns observed here in acetonitrile for oxidation and reduction potentials of homologous 3d, 4d, and 5d transition metal complexes were also found for (α-diimine)M(CO)$_4$ compounds (M = Cr, Mo, W).[16]

Table 2. IR Spectroelectrochemical Data[a]

complex	ν_{CN}		
$[(mpz)Fe(CN)_5]^{2-}$	2095 (s)	2086 (m)	2080(s)
$[(mpz)Ru(CN)_5]^{2-}$	2100 (s)	2084 (w, sh)	2071(s)
$[(mpz)Os(CN)_5]^{2-}$	2105 (s)	2085 (w, sh)	2070(s)
$[(mpz)Ru(CN)_5]^{3-}$	2081 (w)	n.o.	2035 (vs)
$[(mpz)Os(CN)_5]^{3-}$	2080 (w)	2047 (vw,sh)	2024 (vs)

[a] From OTTLE spectroelectrochemistry in DMF/0.1 M Bu_4NPF_6/0.1 M [2.2.2]cryptand. Absorption maxima in cm^{-1}.

Not only the potentials but also the reactivities observed after reduction in acetonitrile are reminiscent of those established for nitrosyl complexes $[(NO)M(CN)_5]^{2-}$ (M = Fe, Ru).[15,17] An EC process[3b] is operating (Scheme 1) in which the "C" step corresponds to the (reversible) dissociation of one cyanide ligand. The extent of dissociation depends on the metal (M = Fe > Ru >> Os), on the presence of cyanide, and on the medium. Even the coordinatively most inert ion in that series, $[(mpz)Os(CN)_5]^{3-}$, disintegrates in acidic aqueous solution. However, the EC dissociation of the mpz$^•$ complexes is slower in comparison to that of corresponding NO$^•$ analogues.[14,15] As demonstrated also for carbonylmetal species,[3b] even the predominantly ligand (L)-centered reduction of a metal complex (L)ML$'_5$ can labilize one of the coligands L$'$ because the occupation of the π* MO of L with one electron is sufficient to diminish M-to-L back-donation. This leaves more negative charge at the ML$'_5$ fragment, which may result in the loss of one σ and/or π donating coligand (16 + δ electron situation).[3b] Stable pentacoordinate species with π acceptor-turned-donor ligands have been observed not only for $[(NO)Fe(CN)_4]^{2-}$ [14,15] and complexes of mpz$^•$ [3b] but also for catecholate/d^6 metal systems.[18]

The paramagnetic cyanometalate(II) complexes (M = Ru, Os) of mpz$^•$ can be reduced further at more negative potentials (Table 1, Scheme 1). Considering the "antiaromatic" 8 π electron nature of two-electron reduced pyrazine derivatives,[19] we cannot make definitive assignments of the structures and oxidation states in these labile species.

IR Spectroelectrochemistry. The presence of well-separated and characteristically split cyanide stretching bands allowed us to study the effect of reduction in the redox systems $[(mpz)M(CN)_5]^{2-/3-}$, M = Ru and Os. The oxidized forms $[(mpz)M(CN)_5]^-$ and the reduced iron complex ion $[(mpz)Fe(CN)_5]^{3-}$ were not sufficiently stable for spectroelectrochemistry with an OTTLE cell, which requires integrity for at least 2 min.

The changes in the cyanide vibrational stretching bands on reducing $[(mpz)Os(CN)_5]^{2-}$ in DMF are illustrated in Figure S1 (Supporting Information). Isosbestic points and the near 100% reappearance of the original spectrum after reoxidation indicate the full reversibility of the conversion. Table 2 summarizes the relevant data.

Three CN stretching bands of different intensity are observed in the IR spectra of the approximately C_{2v}-symmetric ions

---

(16) Ernst, S.; Kaim, W. *J. Am. Chem. Soc.* **1986**, *108*, 3578.

(17) (a) Manoharan, P. T.; Gray, H. B. *J. Am. Chem. Soc.* **1965**, *87*, 3340. (b) Olabe, J. A.; Gentil, L. A.; Rigotti, G.; Navaza, A. *Inorg. Chem.* **1984**, *23*, 4297. (c) Baraldo, L. M.; Bessega, M. S.; Rigotti, G. E.; Olabe, J. A. *Inorg. Chem.* **1994**, *33*, 5890.

(18) (a) Darensbourg, D. J.; Klausmeyer, K. K.; Mueller, B. L.; Reibenspies, J. H. *Angew. Chem.* **1992**, *104*, 1501; *Angew. Chem., Int. Ed. Engl.* **1992**, *31*, 1503. (b) Hartl, F.; Vlcek, A., Jr.; deLearie, L. A.; Pierpont, C. G. *Inorg. Chem.* **1990**, *29*, 1073.

(19) (a) Kaim, W. *Rev. Chem. Intermed.* **1987**, *8*, 247. (b) Kaim, W.; Schulz, A.; Hilgers, F.; Hausen, H.-D.; Moscherosch, M.; Lichtblau, A.; Jordanov, J.; Roth, E.; Zalis, S. *Rev. Chem. Intermed.* **1993**, *19*, 603.

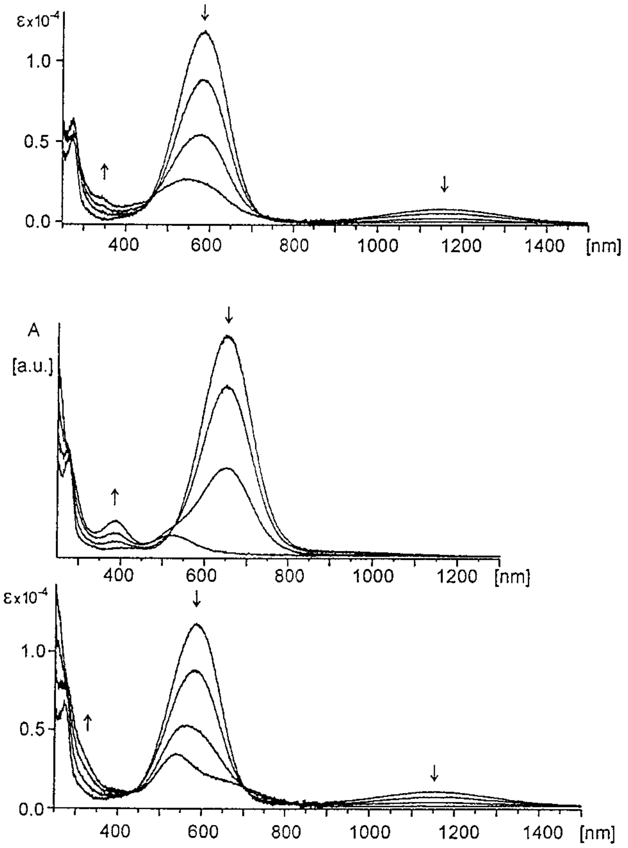

Figure 2. UV/vis/NIR spectroelectrochemistry of the transitions $[(mpz)Os(CN)_5]^{(2-)\rightarrow(-)}$ (top), $[(mpz)Ru(CN)_5]^{(2-)\rightarrow(3-)}$ (center), and $[(mpz)Os(CN)_5]^{(2-)\rightarrow(3-)}$ (bottom) in CH_3CN/0.1 M Bu_4NPF_6/0.1 M [2.2.2]cryptand.

Table 3. Absorption Maxima[a,b] of Complexes

solvent	M = Fe	M = Ru	M = Os		$\Delta\nu$[c]
		$[(mpz)M(CN)_5]^{2-}$			
CH_3CN	713 (14.0)	656 (15.2)	586 (17.1)[d]	1160 (8.6)[e]	8.6
		$[(mpz)M(CN)_5]^{3-}$			
CH_3CN[f]	n.d.	524, 388	680 (sh), 541[g]		
		$[(mpz)M(CN)_5]^{-}$			
CH_3CN[f]	n.d.	n.d.	544,[h] 338[i]		
		$[(mpz)M(NH_3)_5]^{3+}$ [j]			
CH_3CN	n.a.	450 (18.5)	450 (22.2)	1100 (9.1)	13.1
		$[(NO)M(CN)_5]^{2-}$ [h]			
H_2O	394 (25.4) 498 (20.1)	345 (29.0) 435 (23.0)	313 (31.9)	427 (23.4)	8.5

[a] Wavelengths λ_{max} in nm, wavenumbers ν_{max} in 10^3 cm^{-1} (in parentheses). [b] Measurements for $Na_2[Fe(CN)_5(mpz)]$, $K_2[Ru(CN)_5(mpz)]$, and $Na_2[Os(CN)_5(mpz)]$ in CH_3CN in the presence of about 0.1 M [2.2.2]cryptand. [c] Energy difference between both maxima for the Os complex in 10^3 cm^{-1}. [d] log $\epsilon = 4.07$; ϵ in M^{-1} cm^{-1}. [e] log $\epsilon = 2.95$. [f] 0.1 M Bu_4NPF_6/0.1 M [2.2.2]cryptand. [g] log $\epsilon = 3.53$. [h] log $\epsilon = 3.43$. [i] log $\epsilon = 3.06$. [j] From ref 7a. [k] From ref 17.

$[(mpz)M(CN)_5]^{n-}$. The three homologues (M = Fe, Ru, Os) show little variation in the 2− state. On reduction to the 3− form for M = Os, both the ν(CN) axial (highest wavenumber) and ν(CN) equatorial modes shift to lower values, as expected from stronger back-donation to the CN^- ligands on going from π-accepting mpz^+ to the possibly even π-donating $mpz^{\bullet}$. However, such effects cannot be correlated quantitatively with oxidation state or geometry changes.[20] Intensity changes may be related to different solvation of these charged species which affect the dipole moments and thus the IR band intensities. The information on the ruthenium compound is limited (only two bands observable) and does not allow us to distinguish between a pentacyano or tetracyano complex (Scheme 1), i.e. a hexa- or pentacoordinate species.[3b]

UV/Vis/NIR Spectroscopy. The visible absorption spectra of the $[(mpz)M(CN)_5]^{2-}$ ions are dominated by intense MLCT bands with shoulders at the low-energy side. For M = Os, the two transitions appear as well-defined bands (Figure 2). The low-energy component can be attributed to a ^{3}MLCT transition, considering the high spin−orbit coupling constant of Os(II).[21] Strong solvatochromic changes were observed in different solvents (see Supporting Information, Table S1 and Figure S2). Although excess [2.2.2]cryptand had to be added for all solvents except water, the MLCT absorption energies correlate very well with Gutmann's acceptor number, AN (Figure S2).[22,23] Stronger accepting solvents cause a stabilization of the metal d orbitals through interaction with the coordinated cyanides and thus lead to hypsochromic shifts in all cases observed (negative solvatochromism[22]). For the main MLCT band the solvent sensitivity increases in the order M = Fe < Os < Ru (Figure S2). The rather small solvatochromic responses of the iron and osmium complexes may be attributed to energetically close-lying ligand π^* and metal d_π orbitals (Fe) or strong orbital mixing (Os). However, the most pronounced solvent dependence is observed for the separate low-intensity long-wavelength band (MLCT2) of the osmium compound (Figures 2 and S2); this phenomenon can be tentatively interpreted as different solvation of ^{1}MLCT and ^{3}MLCT excited states and is under current investigation.

The UV/Vis spectroelectrochemical results (Figure 2, Table 3) illustrate that the MLCT bands are diminished in intensity and shifted to higher energies, both on oxidation and reduction. The lowered intensities (Figure 2) of the MLCT bands follow from half-occupied MOs involved in the transition and from diminished metal/ligand orbital overlap. Intraligand transitions of pyrazinium radicals are expected to be very weak[19b] when compared to MLCT features. Isosbestic points and the reappearance of spectra after re-reduction or reoxidation confirm the reversibility of the processes for the osmium systems. However, the isosbestic point appears only at the beginning of the reduction of $[(mpz)Ru(CN)_5]^{2-}$, and a slow conversion occurs on the time scale of 5−10 min after reduction, suggesting cyanide dissociation[15] (Scheme 1). The slower dissociation of $[(mpz)Ru(CN)_5]^{3-}$ as compared to that of the iron analogue but higher reactivity relative to the inert $[(mpz)Os(CN)_5]^{3-}$ parallels the relative rates of pyrazine release from the $[M(CN)_5pz]^{3-}$ ions (M = Fe, Ru, Os).[8]

EPR Spectroscopy. The one-electron reduced forms obtained from precursor ions $[(mpz)M(CN)_5]^{2-}$ exhibit at least partially resolved EPR spectra at room temperature (Figures 3 and S3). Excluding metal isotope and cyanide N coupling, the hyperfine structure of *N*-methylpyrazinium radicals[3,6c,7d] $mpz^{\bullet}$ involves five coupling parameters (2 × 2 C*H*, 1 C*H*$_3$, 2 N) with a total of 324 theoretical lines. Spectral analysis (Tables 4 and S2) showed that hyperfine splitting from the ^{14}N nuclei ($I = 1$) of the cyanide ligands is not observed here, which confirms

---

(20) (a) Kaim, W.; Bruns, W.; Kohlmann, S.; Krejcik, M. *Inorg. Chim. Acta* **1995**, *229*, 143. (b) Atwood, C. G.; Geiger, W. E. *J. Am. Chem. Soc.* **1993**, *115*, 5310.

(21) (a) Kober, E. M.; Meyer, T. J. *Inorg. Chem.* **1982**, *21*, 3966. (b) Johnson, S. R.; Westmoreland, T. D.; Caspar, J . V.; Barqawi, K. R. *Inorg. Chem.* **1988**, *27*, 3195. (c) Lay, P. A.; Magnuson, R. H.; Taube, H. *Inorg. Chem.* **1988**, *27*, 2364.

(22) Reichardt, C. *Solvent and Solvent Effects in Organic Chemistry*, 2nd. ed.; Verlag Chemie: Weinheim, Germany, 1988.

(23) Gutmann, V.; Resch, G.; Linert, W. *Coord. Chem. Rev.* **1982**, *43*, 133.

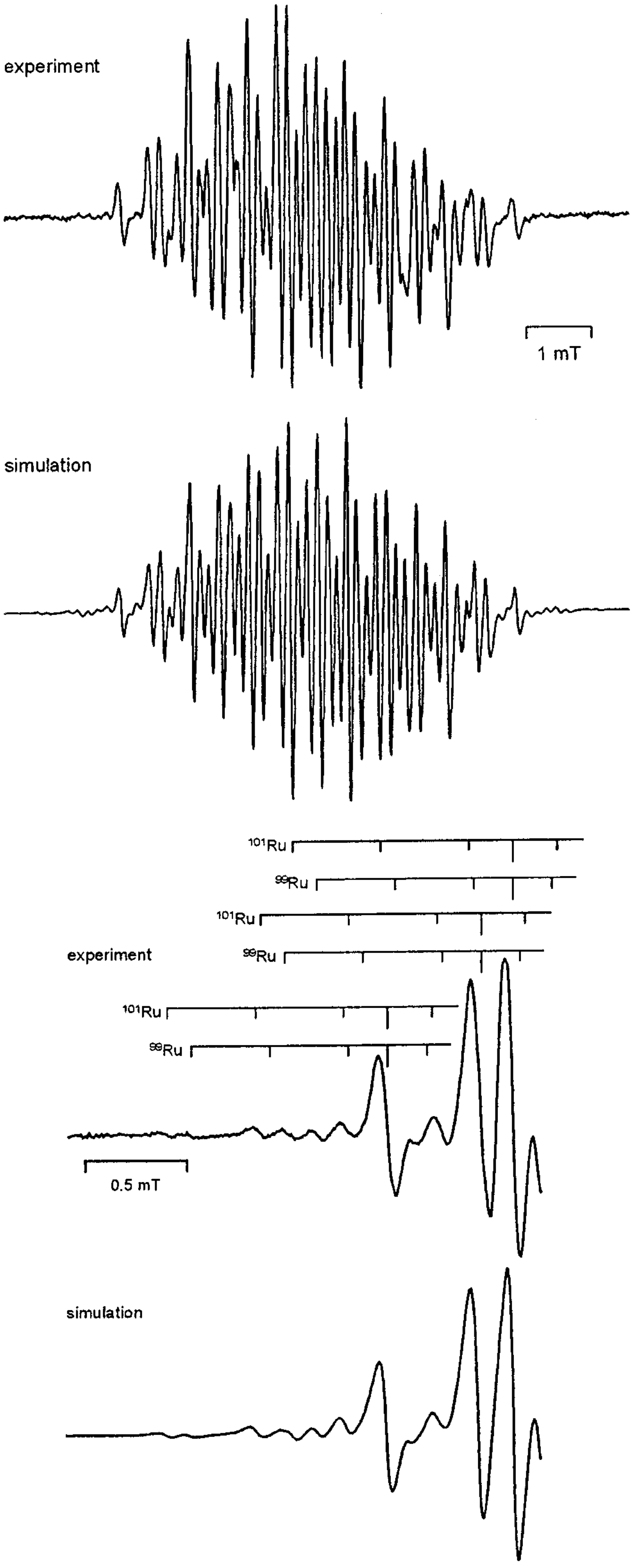

Figure 3. EPR spectrum and computer simulation of the radical species obtained from $K_2[(mpz)Ru(CN)_5]$ by cathodic reduction in CH_3CN/0.1 M Bu_4NPF_6/0.1 M [2.2.2]cryptand (top and center). The amplified low-field section shows resolved separate coupling from ^{99}Ru and ^{101}Ru isotopes in natural abundance (bottom).

Table 4. EPR Data[a] for $mpz^\bullet$ and Its Complexes $mpz^\bullet{-}X$

	a						*a*(CH)	
X	$H^{2,6}$	$H^{3,5}$	CH_3	N^1	N^4	*g*	Δ[b]	Σ[c]
[d]	458	121	732	700	828	2.0034	337	579
H^+ [e]	310	292	851	891	705	2.0034	18	602
$[Ru(NH_3)_5]^{2+}$ [f]	387	<180	723	683	870	2.0021	>207	<567
$W(CO)_5$[g]	386	154	714	784	870	2.0051	232	540
$Mo(CO)_3(R_3P)$[h]	409	87	646	738	846	2.0041	322	496
$W(CO)_3(R_3P)$[g]	394	77	617	709	862	2.0087	317	471
$[Fe(CN)_4]^{2-}$ [i]	475	84	703	705	811	2.0034	391	559
$[Ru(CN)_4]^{2-}$ [j]	452	<30	624	760	895	2.0061	>420	<480
$[Os(CN)_5]^{3-}$ [k]	≈550		≈550			2.0157		

[a] Coupling constants *a* in μT. Assignments to N^1 or N^4 uncertain. [b] Difference of coupling constants for protons $H^{2,6}$ and $H^{3,5}$. [c] Sum of coupling constants for protons $H^{2,6}$ and $H^{3,5}$. [d] From ref 6c. [e] From ref 26. [f] From ref 7d; $a(^{99}Ru) = 580$ μT, $a(^{101}Ru) = 650$ μT. [g] From ref 3a. [h] From ref 3b; $a(^{95,97}Mo) = 315$ μT. [i] This work; from electrolysis of $[(mpz)Fe(CN)_5]^{2-}$ in DMSO/0.1 M Bu_4NPF_6/0.1 M [2.2.2]cryptand. [j] This work; from electrolysis of $[(mpz)Ru(CN)_5]^{2-}$ in CH_3CN/0.1 M Bu_4NPF_6/[2.2.2]cryptand. Additional resolved coupling: $a(^{99}Ru) = 390$ μT, $a(^{101}Ru) = 437$ μT. [k] This work; from electrolysis of $[(mpz)Os(CN)_5]^{2-}$ in CH_3CN/0.1 M Bu_4NPF_6/[2.2.2]cryptand.

the predominant localization of spin at the mpz ligand. The previously reported[6c] iron system was also reinvestigated, in view of the electrochemical evidence for dissociation (Scheme 1).

Using the radical generation technique described previously,[6c] we also reacted the precursor ions $[(mpz)M(CN)_5]^{2-}$ with dithionite $S_2O_4^{2-}$ in concentrated aqueous KOH. EPR spectra obtained from these aqueous solutions or from dichloromethane solutions after extraction[6c] showed rather narrow lines (Figure S3), *g* factors close to the free ligand value of 2.0034, relatively similar but not completely identical coupling constants (Table S2), and no detectable metal hyperfine splitting. The identity of these radical species is thus uncertain, and they will not be discussed further; one alternative assignment is that of rather loosely associated and solvated pairs $mpz^\bullet/[M(CN)_x]^{2-x}$.

In contrast, the species generated electrolytically in DMSO or CH_3CN from $[(mpz)M(CN)_5]^{2-}$ exhibit the expected effects of heavy metal coordination to a radical:[5,7d,10] The dissociatively inert complex $[(mpz)Os(CN)_5]^{3-}$ shows an insufficiently resolved EPR spectrum which allowed us to determine only one coupling constant $a \approx 0.55$ mT at the outermost section of the spectrum. Substitution of 3d or 4d transition metals by the much heavier 5d analogues in radical complexes is well-known to cause an increase of the EPR line width[10] because of slower tumbling motion in solution and thus insufficient averaging of anisotropic contributions from the **g** and **A** tensors. Sizable contributions from the coordinated 5d metal are also evident from the rather large g_{iso} value of 2.0157, reflecting the high spin−orbit coupling constant of osmium.[24]

The well-resolved EPR spectrum of the cathodically generated ruthenium species could be fully analyzed, including *separate* features from ^{99}Ru and ^{101}Ru metal isotope hyperfine splitting (Figure 3, Table 4). In addition to the *g* factor of 2.0061, these observations clearly indicate an oligo(cyanoruthenium(II)) complex of the *N*-methylpyrazinium radical. The coordinated ruthenium isotopes ^{99}Ru (12.7% natural abundance, $I = {}^5/_2$) or ^{101}Ru (17.0%, $I = {}^5/_2$) give rise to hyperfine interactions with the unpaired electron, the ratio of coupling constants (Table 4) following the literature ratio of 1.12 in favor of ^{101}Ru for the nuclear magnetic moments.[24] Following the results from UV/vis spectroelectrochemistry and considering the time of about 10 min required for *intra muros* radical generation and EPR measuring, we identify the observed species as the cyanide dissociation product $[(mpz)Ru(CN)_4]^{2-}$. Some of the mpz hyperfine splitting parameters of $[(mpz)Ru(CN)_4]^{2-}$ are quite distinct, such as the small values for *N*-methyl protons and $H^{3,5}$ nuclei and the relatively large coupling constant of N^1 (Table 4).

---

(24) (a) Goodman, B. A.; Raynor, J. B. *Adv. Inorg. Chem. Radiochem.* **1970**, *13*, 135. (b) Weil, J. A.; Bolton, J. R.; Wertz, J. E. *Electron Paramagnetic Resonance*; Wiley: New York, 1994.

The paramagnetic product observed by EPR after the *intra muros* one-electron reduction of $[(mpz)Ru(CN)_5]^{2-}$ in acetonitrile is thus ascribed to the pentacoordinate[3b] species $[(mpz^\bullet)Ru^{II}(CN)_4]^{2-}$. No such dissociation was observed for the osmium analogue $[(mpz)Os(CN)_5]^{3-}$ whereas the electrochemical irreversibility of the reduction of $[(mpz)Fe(CN)_5]^{2-}$ (Figure 1) clearly indicates that the postulated[6c] $[(mpz)Fe(CN)_5]^{3-}$ species is *not* the observed paramagnetic product. Instead, we assign the reproduced spectrum from the electrochemical reduction of $[(mpz)Fe(CN)_5]^{2-}$ in DMSO to the EC dissociation product $[(mpz)Fe(CN)_4]^{2-}$ (Scheme 1, Table 4). The hyperfine values of that species are less unusual than those of $[(mpz)Ru(CN)_4]^{2-}$ and the isotropic g factor is lower, in agreement with the smaller spin−orbit coupling constant of iron.[24]

Remarkably, the EPR spectrum of the ruthenium radical complex revealed *separate* satellite hyperfine coupling features from the ^{99}Ru and ^{101}Ru isotopes (390 and 437 μT) which conform to the natural abundances and the ratio of nuclear magnetic moments. Relative to the isotropic hyperfine coupling constants A_{iso} for ^{99}Ru ($A_{iso} = -62.94$ mT) and ^{101}Ru ($A_{iso} = -70.52$ mT)[24b] the measured values amount to about 0.62%, which indicates[10] a small but non-negligible spin transfer from the heterocyclic radical ligand. Slightly higher values had been reported for $[(mpz)Ru(NH_3)_5]^{2+}$ [7d] (580 and 650 mT, Table 4) and for the tetracyanoruthenate(II) chelate system $[(bpz)Ru(CN)_4]^{3-}$ (458 and 514 mT, bpz = 2,2′-bipyrazine);[25] in both cases the two isotope hyperfine features were not observed separately but calculated in spectra simulation procedures.

In agreement with the observation of metal isotope hyperfine splittings in the case of $^{99,101}Ru$ there is a characteristic perturbation of the spin distribution within the $mpz^\bullet$ heterocyclic π system (Table 4). Whereas the two ^{14}N coupling constants differ only by about 20%, the pyrazine ring protons $H^{2,6}$ and $H^{3,5}$ reflect more distinctly the asymmetry between coordination of the acceptor substituent H_3C^+ at N^1 and of the donor fragment $[(NC)_4Ru]^{2-}$ at N^4. In fact, the compilation in Table 4 illustrates that this asymmetry[5] Δa(CH) is quite large for the complexes of the tetracyanometalate(II) species described here, larger than in uncoordinated *N*-methylpyrazinium free radical or other complexes.

The sum $\sum$a(CH) of pyrazine ring proton coupling constants reflects the delocalization of spin to the peripheral N^4-coordinated metal fragments. Smaller $\sum a$(CH) values indicate a higher degree of mpz-to-metal spin delocalization. This delocalization seems relatively small for the fragment $[(NC)_4Fe]^{2-}$ in comparison to that of $[(NC)_4Ru]^{2-}$ or phosphine-containing Mo^0 or W^0 species;[3] unfortunately, the poor EPR resolution of the pentacyanoosmium species does not allow us to make a corresponding statement.

However, the rather high g factors of both the paramagnetic Ru and Os complexes (Table 4) suggest considerable mixing of metal d and mpz ligand π^* orbitals. According to an approximation (Scheme 2),[10] the factors determining g include the spin−orbit coupling constant ξ of the atoms contributing to a significant extent to spin (de)localization because of the admixture of higher magnetic states with nonzero angular momentum to the radical ground state. It can thus be anticipated that the radical complex with the 5d transition element osmium ($\xi \approx 2500$ cm^{-1}) exhibits a much larger deviation Δg from the values for the free electron ($g_e = 2.0023$) or the free ligand radical ($g = 2.0034$)[3] than the complex of the 4d analogue, ruthenium ($\xi \approx 1000$ cm^{-1}).[24]

Scheme 2

$$\Delta g = g - g_e = k\xi\left(\frac{1}{\Delta E_1} - \frac{1}{\Delta E_2}\right)$$

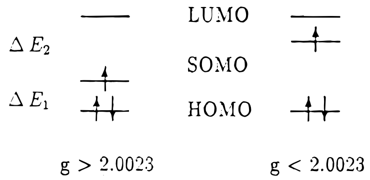

The magnitude and sign of Δg are also affected by the energy differences to neighboring states. In a simple one-electron orbital picture,[10] small g values as for $[(mpz)Ru(NH_3)_5]^{2+}$ indicate low-lying unoccupied MOs close to the singly occupied MO (SOMO) whereas the comparatively (Table 4) high g values for $[(mpz)M(CN)_n]^{2-n}$ suggest occupied MOs close to the π^* SOMO and a large gap to unoccupied molecular orbitals. In addition to the larger ligand field exerted by CN^- relative to NH_3, this result points to some stabilization of the π^*(mpz) orbital in $[(mpz)M(CN)_n]^{2-n}$ despite the negative charge; on the other hand, stronger d(M)/π^*(mpz) orbital mixing[7b] in $[(mpz)Ru(NH_3)_5]^{2+}$ leads to a destabilized π^*(mpz) MO as is evident from lower g and larger metal hyperfine values (Table 4).[7d]

Summarizing, by using a number of different spectroscopic and spectroelectrochemical approaches, we could establish that there is at least a qualitative similarity between the $NO^{+/\bullet}$ and $mpz^{+/\bullet}$ ligand redox systems in their coordination compounds with $[M(CN)_n]^{2-n}$ metal fragments. This is based on the low σ-donor and strong π-acceptor abilities of both ligands; mpz^+ lies at the extreme of the series of pyridine and pyrazine derivatives in $[M(CN)_5L]^{n-}$, showing significant shifts in infrared ν(CN), MLCT transition energies and intensities, and M−N (heterocycle) distances. All these indicators reflect a high degree of $M^{II}-mpz^+$ back-bonding interaction but also show that this is still lower than in the $M^{II}-NO^+$ bond. The observed differences, e.g. more pronounced EC reactivity and spectroscopic shifts of the NO analogues, can be attributed to the smaller π system which supports a higher degree of π back-donation in nitrosyl complexes. Furthermore, the higher symmetry of NO allows for a different electronic structure[17] due to the degeneracy of orbitals.

Acknowledgment. This work was made possible through a grant from GTZ, Eschborn, Germany. We also gratefully acknowledge support from Deutsche Forschungsgemeinschaft and Volkswagenstiftung and from the University of Buenos Aires. J.A.O. is a member of the research staff of Conicet (Argentina).

Supporting Information Available: Figures showing the IR spectroelectrochemistry of $[(mpz)Os(CN)_5]^{(2-)\to(3-)}$ (Figure S1), correlations between the acceptor numbers of solvents and the wavenumbers of MLCT absorption maxima for $[(mpz)M(CN)_5]^{2-}$ (M = Fe, Ru, Os) (Figure S2), and EPR spectra of paramagnetic species obtained from $Na_2[(mpz)Fe(CN)_5]$ by various radical generation techniques (Figure S3) and complete tables listing data concerning solvatochromism (Table S1) and EPR spectroscopy (Table S2) (8 pages). Ordering information is given on any current masthead page.

IC961426A

---

(25) (a) Waldhör, E.; Poppe, J.; Kaim, W.; Cutin, E. H.; Garcia Posse, M.; Katz, N. E. *Inorg. Chem.* **1995**, *34*, 3093. (b) Slightly different data based on less resolved spectra were reported later: Samuels, A. C.; DeArmond, M. K. *Inorg. Chem.* **1995,** *34*, 5548.

(26) Kaim, W. *J. Chem. Soc. Perkin Trans. 2* **1984**, 1357.